INTERNATIONAL JOURNAL OF INTEGRATED ENGINEERING
ISSN: 2229-838X e-ISSN: 2600-7916

IJIE

Vol. 17 No. 6 (2025) 97-109
https://publisher.uthm.edu.my/ojs/index.php/ijie

Enhanced Performance of Millimetre-Wave Dual-Polarized Antennas Through Reduced Element Spacing

Siti Zainab Mohd Hamzah[1], Norun Farihah Abdul Malek[1]*, Sarah Yasmin Mohamad[1], Farah Nadia Mohd Isa[1], Athirah Mohd Ramly[2]

[1] *Microwave, Communication, and Information System Engineering (MCISERG), Kulliyyah of Engineering, International Islamic University Malaysia, Jalan Gombak, 53100 Kuala Lumpur, MALAYSIA*

[2] *Department of Computing and Digital Technologies, School of Architecture, Computing, and Engineering, University of East London, London E16 2RD, UNITED KINGDOM*

*Corresponding Author: norun@iium.edu.my
DOI: https://doi.org/10.30880/ijie.2025.17.06.008

Article Info

Received: 18 March 2025
Accepted: 24 October 2025
Available online: 30 December 2025

Keywords

Millimetre-waves, dual-polarized, patch antenna, inter-elements spacing

Abstract

The demand for higher data rates and improved signal quality in 5G wireless networks has led to the development of dual-polarized antennas, offering enhanced channel capacity and MIMO performance. However, challenges such as isolation, compactness, and beamforming persist, particularly in millimeter-wave applications. This study presents an improved single-layer, dual-polarized slant ±45° patch antenna with reduced inter-element spacing at 28 GHz, aiming to optimize antenna performance while maintaining a compact design. The proposed antenna is designed using Rogers RT5880 substrate and features a T-power divider for efficient signal distribution. Performance evaluations, including simulations and experimental measurements, demonstrate enhanced reflection coefficient, radiation patterns, and gain compared to previous designs. The inter-elements spacing is reduced from approximately 57 mm to 15 mm. The results indicate that reducing inter-element spacing effectively minimizes sidelobe levels and improves radiation pattern, making this antenna suitable for 5G millimeter-wave applications. The measured reflection coefficient achieves less than -10 dB, which is a good performance. The measured patterns fall between the range of 3.7 to 7.8 dBi. The radition patterns of improved antenna have less sidelobes and the co-elevation azimuth pattern has more directional main beam pattern compared to the previous antenna. For future works, this feature makes it suitable for 5G's millimetre-waves beam-steering applications.

1. Introduction

Increasing demand in data rate transfer and wide signal coverage offered by 5G wireless technology has opened many alternatives such as implementing dual polarization diversity. The most common advantages of dual polarization diversity to the 5G antenna are increased channel capacity, improved signal quality, and enhanced MIMO performance [1] [2]. However, it also comes with several challenges such as isolation, compactness, beamforming and coverage [3]. Ensuring high isolation of inter-element ports is crucial to reduce the side lobe levels and enhance the antenna system performance [4]. Integrating dual-polarized antennas into small devices like smartphones while maintaining performance is challenging due to limited space. These isolation and compactness of 5G's antenna feature have become a trade-off to improve the quality of antenna's transmission signals.

For the past researches, the most common type of antenna used to realize dual polarization feature is dipoles due to ease to configure [5] [6]. However, one of the obvious characteristics of dipoles is omnidirectional pattern which is suitable for base station applications. It is quite challenging to achieve unidirectional radiation pattern in favour to 5G's demand. This also explains the patch antenna is chosen due to its characteristics of ease of fabrication, non-complex architecture, and able to achieve directional high gain pattern.

Polarization diversity is well known to be an efficient technique improving the reliability of wireless communication [7]. Polarization diversity is a technique to improve signals quality by reducing interference and it involves using different polarization states of electromagnetic waves for signals transmission. Besides, designing dual-polarized antennas with high gain and beamforming capabilities for wide signal coverage is complex especially at millimetre-wave frequencies where signals are more directional and prone to blockages. A pair of slot antenna arrays arranged with a 90° difference on a smartphone PCB, operating at 28 GHz reports favourable return loss parameters, radiation patterns, efficiency, and gain making it suitable for 5G mobile terminals [8]. Implementing dual-polarized feature to the Low-Temperature Co-fired Ceramic (LTCC) technology by integrating a horizontally polarized mesh-grid patch with a vertically polarized folded slot antenna has also achieves an impedance bandwidth of 850 MHz at 28 GHz with measured gains of 3.19 dBi and 2.95 dBi for horizontal and vertical polarizations, respectively [9]. Reference [10] covers 5G bands by excites two orthogonal modes in substrate integrated waveguide (SIW) cavity, exhibiting wide bandwidths and symmetric radiation patterns. A parasitic element improves port-to-port isolation and guides the main beam. These studies highlight advancements in dual-polarized antenna designs tailored for 28 GHz 5G applications, focusing on aspects like bandwidth, gain, isolation, and integration suitability for mobile devices.

Antennas with dual linear slant ±45° polarization are also capable to offer wide bandwidth from 1.7 to 2.7 GHz [11]. Reference [12] has proposed a multilayer slant polariser to change the direction of antenna's polarization and it also offers wide bandwidth from 6.5 to 18 GHz. Similar to reference [13] and [14] which achieve 75.9% and >36% bandwidth, respectively. Other than wide bandwidth feature offered by the slant 45° polarization antenna, it also capable to output high gain [15] [16] [17]. This past research carried out investigation on lower frequency antenna. There are several studies investigated on 5G frequency band's antenna, as an example study found in [18], they developed a dual slant ±45° polarized beamforming array using RFIC beamforming chipsets operating from 26 to 30 GHz. Besides, a dual band antenna has also been proposed by [19] to produce high gain from dual slant ±45° Ka-band. Reference [20] also designed a slot-coupled patch antenna with dual slant ±45° to produce high gain. However, these studies developed complex implementation of dual polarization feature to the antenna architecture. Therefore, the previous studies in [21] introduced simplified single-layer dual-polarized antenna using a combination of slanted 45° patch elements to the right and left direction to the normal or reference plane.

Implementation of a single-layer dual slant ±45° polarized antenna for millimetre-wave applications is quite challenging. The major factor is its configuration of elements spacing. Reference [22] has recently developed a single layer ±45° dual-polarized directional array antenna for 30 GHz operating frequency. They used two series-fed ports to excite dual circularly polarized array and radiate in ±45° polarization orientations. Similar to reference [23], they used two series-fed dual circularly polarized at ±45° polarized radiation by using phase control approach.

Dual-polarized antennas are a cornerstone of 5G technology, addressing the growing demand for faster, more reliable, and efficient wireless communication. Despite challenges, advancements in materials, design techniques, and integration with emerging technologies make them a pivotal component of modern and future communication systems. This work introduces a simpler and more compact design for a dual-polarized patch antenna operating at 28 GHz for 5G applications. The main improvement is the significant reduction in spacing between the antenna elements, from 57 mm in the previous design [21] to just 15 mm, which helps reduce sidelobes and produce a more focused directional main beam pattern. In addition, an improved T-power divider is used, allowing for better signal distribution and improved impedance matching. As a result, the antenna achieves better simulated reflection coefficient improved from –11 dB to –17 dB and higher simulated gain performance, while still maintaining good measurement results. The antenna also supports dual ±45° polarization using only a single feed port, making it more compact, easier to fabricate, and well-suited for future 5G beam-steering applications.

Therefore, in this study, a simple design of a single-layer antenna structure at 5G millimetre-waves is developed with dual-polarized slant ±45° polarizations to offer the flexibility of dual signals transmission simultaneously with only one feeding port. The first section describes the advantages of polarization diversity to the 5G's millimetre-waves, the past research on complex dual-polarized antenna designs or structures, and also the dual-polarized slanted ±45° antenna for millimetre-waves applications. The second section explains the antenna simulation design, T-power divider, and fabricated antenna. The third section describes the experimental setup for reflection coefficient, radiation patterns and gain measurement of the antenna. The last section shows the comparison between simulated and measured results of the antenna in previous work [21] and the improved antenna.

Int. Journal of Integrated Engineering Vol. 17 No. 6 (2025) p. 97-109

2. Antenna Design

In this design, the material chosen is Rogers RT5880 with a dielectric constant of 2.2, loss tangent of 0.0009, and thickness of 1.575 mm. The width and length of the radiating patch elements, substrate and its ground plane are calculated based on equations (1-5) [21]. Based on this previous work in [21], the combination of edge coaxial feeding and corporate feed was used to realize dual polarized ±45°. However, in this work, the T-power divider with edge coaxial feeding is used based on (6) and also in [24] [25] [26].

A modification was made to the T-power divider by reducing the length between the two output ports to improve the main beam pattern. The overall dimension of the T-power divider, width and length of the substrate and ground plane are also changed into a smaller size. The dimension of the patch elements is fixed similar as the previous antenna as shown in Fig. 1.

The dimension of W_P and L_P are calculated using Eq. (1-5) [ref]. However, the design is a standard patch antenna design. Later, the design has been rotated to ±45° to achieve dual slant polarization [21]:

$$W = \frac{\lambda_0}{2\sqrt{0.5(\varepsilon_r + 1)}} \tag{1}$$

W is the width of the patch, λ_0 is the wavelength of antenna's operating frequency, and ε_r is the dielectric constant of the material.

For (W/h>1)

$$\varepsilon_{eff} = \frac{\varepsilon_r + 1}{2} + \frac{\varepsilon_r - 1}{2}\left(\frac{1}{\sqrt{1 + 12h/W}}\right) \tag{2}$$

ε_{eff} is the effective permittivity and h is the thickness of the substrate.

The length extension, ΔL:

$$\Delta L = 0.412h\frac{\left(\varepsilon_{eff} + 0.300\right)\left(\frac{W}{h} + 0.264\right)}{\varepsilon_{eff} - 0.258\left(\frac{W}{h} + 0.813\right)} \tag{3}$$

Then, the length of the patch, L can be calculated as:

$$L = \frac{c_0}{2f_r\sqrt{\varepsilon_{eff}}} \tag{4}$$

$$L_{eff} = L - 2\Delta L \tag{5}$$

where L is the length of patch before fringing correction and L_{eff} is the length of patch after fringing correction.

$$Z = Z_{out}\sqrt{N} \tag{6}$$

where Z is the required impedance value depends on the number of antenna elements, Z_{out} is the input impedance of the feeding line antenna, and N is the number of elements of antenna.

It is important to design directional beam pattern antenna for millimetre-waves applications and it is required to have a clear visible directional main beam to achieve good quality of signals transmission [27]. Therefore, the T-power divider is used to combine patch elements of the antenna by reducing the spacing between elements. Inter-elements spacing is crucial as it may decrease the sidelobe levels and improve the directivity as well as its gain [28]. The patch elements and T-power divider are designed using the CST Simulation tool as depicted in Fig. 1. The simulated T-power divider is shown in Fig. 2 and the fabricated antenna with the SMA feeding connector is shown in Fig. 3. Table 1 lists the parameters of the patch elements and T-power divider.

The antenna design depicted in Fig. 1 is based on fundamental microstrip patch antenna theory, where the patch dimensions are calculated to achieve resonance at 28 GHz using Rogers RT5880 substrate (ε_r = 2.2). Dual-polarization is implemented by orienting the two patch elements at slant ±45° angles relative to the reference plane, allowing excitation of orthogonal linear modes to reduce mutual coupling and enhance polarization

diversity. The reduced inter-element spacing, minimized from 57 mm to 15 mm, is guided by antenna array theory to suppress grating lobes and lower mutual coupling, which directly improves the reflection coefficient (S_{11}). Additionally, the use of a compact T-power divider ensures balanced power splitting while maintaining impedance matching between the feed and patch elements, further contributing to the observed low S_{11} (< −10 dB). This integrated approach aligns with established antenna design principles, resulting in improved radiation performance suitable for 5G millimeter-wave applications.

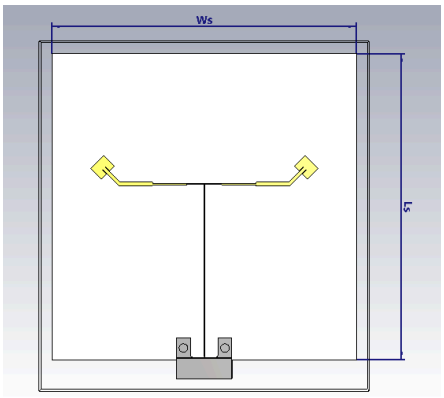

(a)

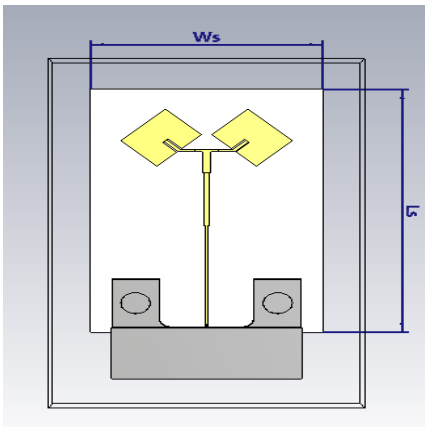

(b)

Fig. 1 *Antenna design of the patch elements and T-power divider of (a) previous antenna; and (b) improved antenna*

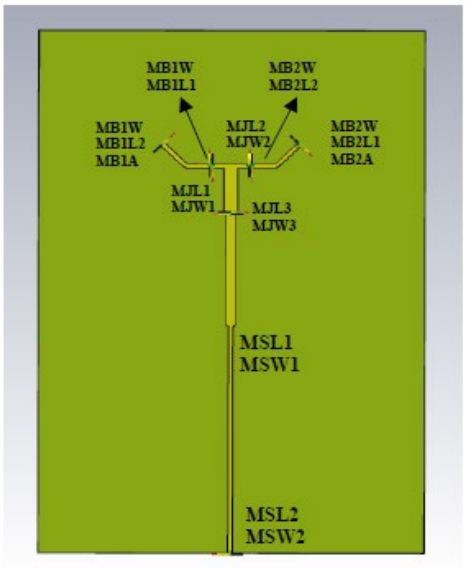

Fig. 2 *The simulated T-power divider*

Int. Journal of Integrated Engineering Vol. 17 No. 6 (2025) p. 97-109

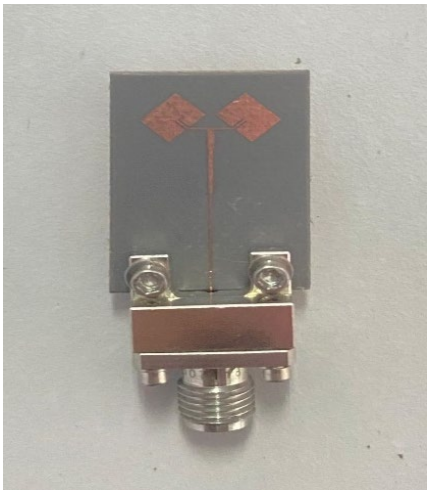

Fig. 3 *The fabricated antenna with feeding connector*

Table 1 *The dimension of patch elements and T-power divider*

Parameters	Dimension (mm)
Width of patch	4.20
Length of patch	3.40
Width of substrate and ground, Ws and Wg	15.65
Length of substrate and ground, Ls and Lg	23.08
Microstrip Step width1 and length1 (MSW1, MSL1)	0.4 and 5.0
Microstrip Step width2 and length2 (MSW2, MSL2)	0.2 and 10.0
Microstrip T junction width1 and length1 (MJW1, MJL1)	0.2 and 0.5
Microstrip T junction width2 and length2 (MJW2, MJL2)	0.2 and 0.5
Microstrip T junction width3 and length3 (MJW3, MJL3)	0.6 and 2.0
Microstrip bend optimal mitered1 width, length1, length2, and angle (MB1W, MB1L1, MB1L2, MB1A)	0.2, 1.0, 1.25, and 45°
Microstrip bend optimal mitered2 width, length1, length2, and angle (MB2W, MB2L1, MB2L2, MB2A)	0.2, 1.25, 1.0, and 45°

3. Measurement Setup

In this section, the antenna on Rogers RT5880 substrate is measured to investigate the performance in terms of reflection coefficient, radiation patterns, and gain.

3.1 Reflection Coefficient

The simulated reflection coefficient is obtained through simulation on CST tool and then it is measured by VNA at the Antenna Laboratory, Malaysian-Japan International Institute of Technology, Universiti Teknologi Malaysia (MJIIT-UTM), Kuala Lumpur, to obtain measured results. Before the measurement is taken place, it is necessary to perform calibration on VNA using a common approach called SOL (Short/Open/Load). VNA calibration seeks to eliminate systematic inaccuracies from the instrument's hardware and account for any elements that may have been introduced to facilitate particular measurements at the necessary frequencies.

The measurement setup is similar to the calibration setup excepts; the female adapter is interconnected to the port cable of VNA and port of the antenna. The reflection coefficient measurement requires one connected cable port. The range of frequencies measured is between 27 and 29 GHz.

3.2 Radiation Pattern and Gain

The antenna is measured in an anechoic chamber at the Antenna Laboratory MJIIT. Before proceeding to the antenna pattern measurement, it is important to identify first the polarization of the antenna from the CST simulation for correct measurement setup. During radiation pattern measurement setup for the antenna, the antenna is placed on top of the antenna holder. Therefore, to attain both co- and cross-polarization of *E*- and *H*-field pattern, the antenna placement must be checked properly. The co- and cross-polarization signals are determined by placing the horn antenna in the same or different polarization to the AUT. The antenna under test (receiver) will rotate 360° to measure the antenna pattern.

Prior to antenna pattern measurement, calibrating the measurement setup is necessary to ensure that the other factors that may affect the measurement are minimized [29], as examples, factors such as range-length loss, reference antenna gain, cable losses, and others. The calibration is done using a reference antenna in this study, a standard gain horn antenna (for 28 GHz operating frequency). The reference horn antenna is placed at the centre of the antenna holder as the AUT and adjusted to be at bore-sight level with the receive antenna. The objective of the calibration is to ensure that a single input signal delivered to the system arrives with equal magnitude and phase at each antenna port.

If the antenna and source cable are ideally matched, all power provided to the antenna will radiate, according to the Friis transmission equation formula [30]. However, the most typical scenario is that there will be impedance mismatched. The calibration measurement setup should be carried out with all wires connected, and the calibration and antenna pattern measurements should both be performed using the same configuration. The total measurement uncertainty will grow if independent calibrations are performed on each component of the system. When possible, it is best to calibrate the system as a whole.

Figs. 4 and 5 show the orientation of antenna for radiation pattern measurement. For the measurement of the co-polarized *E*-plane pattern, the antenna (receiver) is positioned vertically relative to the normal axis of the antenna holder, as shown in Fig. 4. Meanwhile, for the measurement of the co-polarized *H*-plane pattern, the antenna is rotated 90° horizontally relative to the normal plane of the antenna holder, as shown in Fig. 5. A similar setup is used for the measurement of cross-polarized *E*- and *H*-plane patterns, except that the horn antenna (transmitter) is rotated 90° horizontally relative to the normal plane.

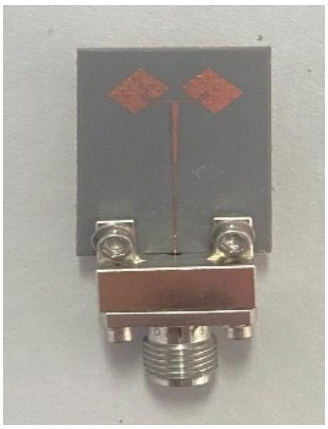

Fig. 4 *Antenna orientation for E-plane pattern measurement*

Int. Journal of Integrated Engineering Vol. 17 No. 6 (2025) p. 97-109

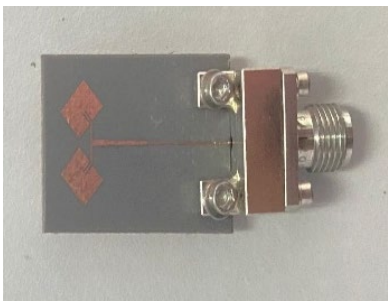

Fig. 5 *Antenna orientation for H-plane pattern measurement*

Fig. 6 shows the whole antenna measurement setup for co-polarized and cross-polarized *E*- and *H*-plane pattern at anechoic chamber. The co-polarized patterns are usually desired patterns to indicate the antenna performance and the cross-polarized patterns are unwanted patterns caused by the mismatch polarization between transmitter and receiver.

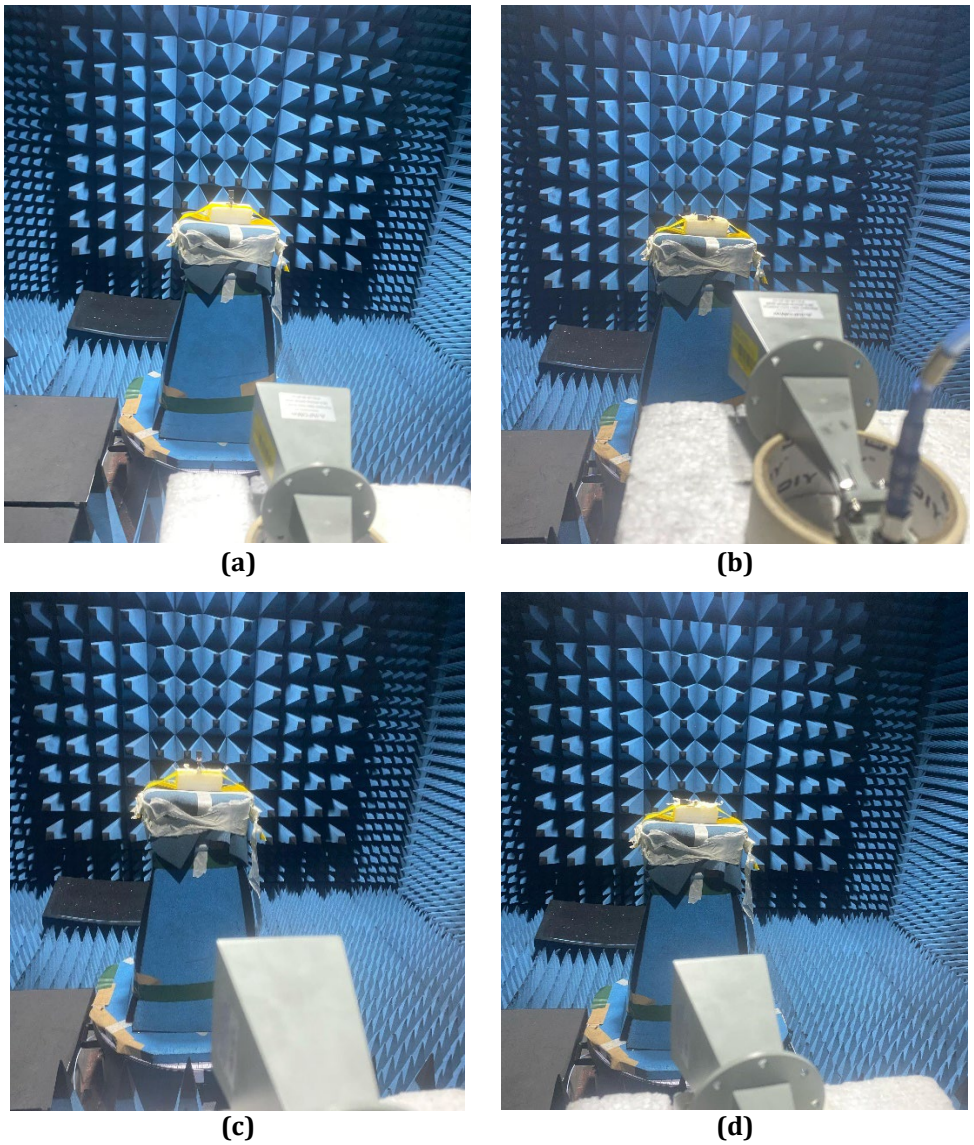

(a) **(b)**

(c) **(d)**

Fig. 6 *The antenna measurement setup of (a) co-polarized E-plane; (b) co-polarized H-plane; (c) cross-polarized E-plane; and (d) cross-polarized H-plane at anechoic chamber*

4. Results and Discussion

Based on the previous dual-polarized slant ±45° antenna [21], the spacing between two patch elements is approximately 57 mm while the dual-polarized slant ±45° antenna in this study reduces its spacing to approximately 15 mm. This section will discuss the effect on reflection coefficient, radiation patterns as well as its gain performance based on the reduced spacing between the patch elements. Both antennas are operating at resonant frequency of 28 GHz. Two subsections below, 4.1 and 4.2 discuss the reflection coefficient, radiation patterns and gain between these two antennas.

4.1 Reflection Coefficient

Fig. 7 shows the simulated and measured reflection coefficient (S_{11}) of the previous dual-polarized antenna and improved dual-polarized antenna. The S_{11} value of previous antenna achieves approximately -11 dB and -12 dB for simulated and measured values at 28 GHz. Meanwhile, the S_{11} value of current antenna achieves -17 dB and -11 dB respectively. Both antennas show a good performance in terms of its reflection coefficient, even though the minimum measured values are slightly shifted from 28 GHz, and the difference of shifting frequency is only by ~0.01 to ~0.03 GHz for both antennas. This is an acceptable occurrence, as the fabrication and drilling process of antenna might influence this shifting frequency. Table 2 lists the simulated and measured values of S_{11} of both antennas.

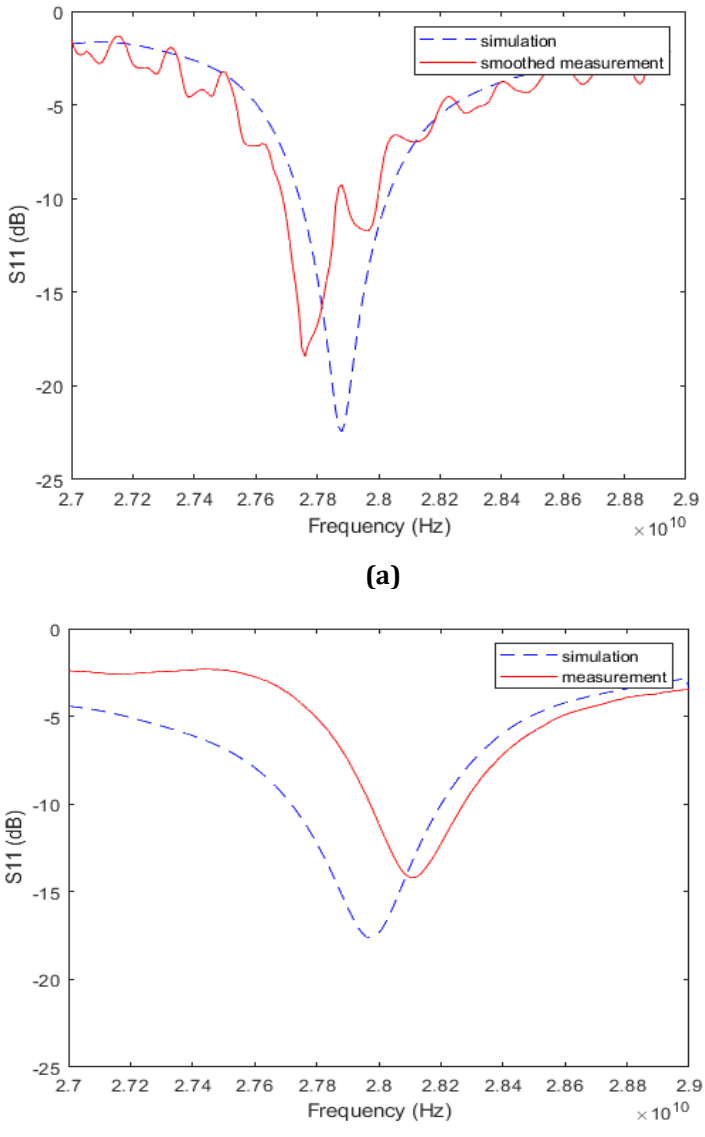

(a)

(b)

Fig. 7 *The reflection coefficient (S_{11}) of (a) the previous; and (b) improved dual-polarized antenna*

Int. Journal of Integrated Engineering Vol. 17 No. 6 (2025) p. 97-109

Table 2 *The simulated and measured S_{11} of both antennas*

Parameters	Simulated S_{11} (dB)	Measured S_{11} (dB)
Previous antenna [21]	-11	-12
Improved antenna	-17	-11

Based on Fig. 7, the simulated S_{11} has been improved by -6 dB. By reducing and optimizing the T-power divider junction dimensions, the impedance transition between the feed line and the dual patches becomes smoother. Besides, by applying 45° mitered bends at the T-junction to reduce reflection due to corner discontinuities [24]. Reference stated by [24] provide theoretical and practical explanations why compact T-junctions improve S_{11} by reducing parasitic and improving impedance transitions. Meanwhile a shifting minimum measured S_{11} is caused by the fabrication and tolerance errors.

4.2 Radiation Patterns and Gain

The previous antenna [21] shows small discrepancies between simulated and measured patterns in terms of its gain; however, the radiation patterns show a similar shape between those simulated and measured patterns at 28 GHz. The simulated patterns for the previous antenna [21] achieve around 2.8 dBi and the measured patterns are 8.7 dBi and 11.1 dBi. The radiation patterns for previous antenna [21] only involve co-polarized patterns. For this study, the normalized 2D polar patterns of improved antenna at 28 GHz are shown in Fig. 8. Table 3 and 4 list the simulated and measured values of gain of both antennas at 28 GHz. Even though the measured results of previous antenna [21] are higher than the improved antenna, there might be some tolerance error due to the man's handling work in antenna placement for measurement. However, from the simulated ones, the improved antenna shows higher gains than the previous one [21]. Besides, the antenna patterns of improved antenna show less sidelobes compared to the previous one [21], and the co-polarized azimuth pattern shows more directional main beam pattern which makes it suitable for 5G's millimeter-wave beam-steering applications.

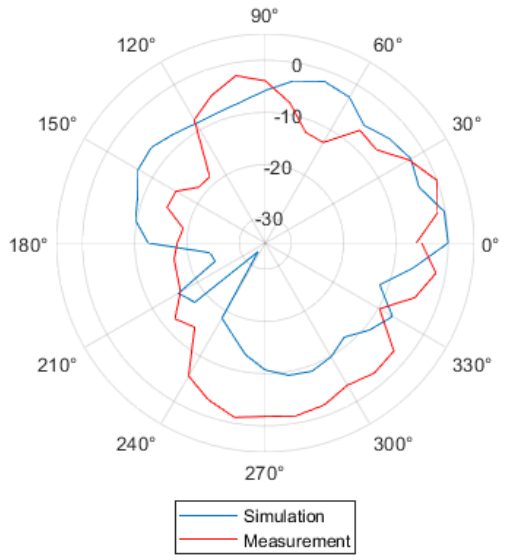

(a)

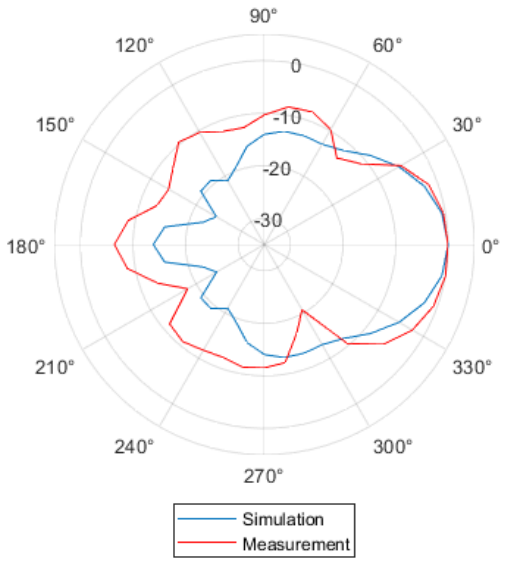

(b)

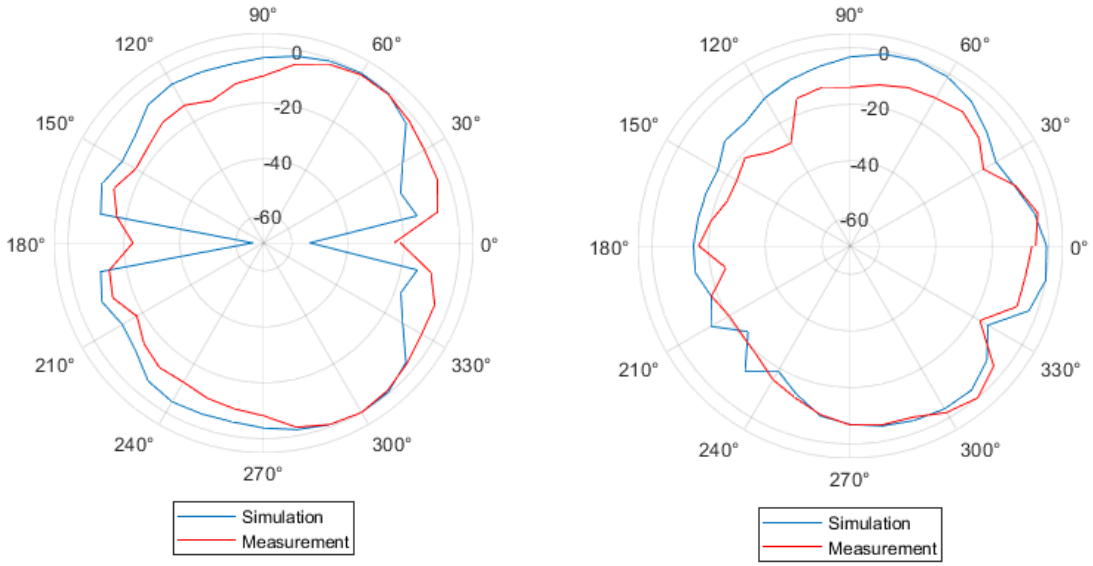

Fig. 8 *The normalized radiation patterns of (a) co-polarized E-plane; (b) co-polarized H-plane; (c) cross-polarized E-plane; and (d) cross-polarized H-plane*

Table 3 *The simulated and measured gain of co-polarized patterns of both antennas*

Antenna	Elevation (E-plane)		Azimuth (H-plane)	
	Simulated S_{11} (dBi)	Measured S_{11} (dBi)	Simulated S_{11} (dBi)	Measured S_{11} (dBi)
Previous antenna [21]	2.8	8.7	2.8	11.1
Improved antenna	7.8	6.7	7.1	3.7

Table 4 *The simulated and measured gain of cross-polarized patterns of antenna*

Antenna	Elevation (E-plane)		Azimuth (H-plane)	
	Simulated S_{11} (dBi)	Measured S_{11} (dBi)	Simulated S_{11} (dBi)	Measured S_{11} (dBi)
Improved antenna	-1.1	-0.5	7.8	3.7

Phased array antenna design for millimeter-wave applications aims to combat high path loss and enhance beam coverage. At the same time, a compact antenna design is essential to support large-scale arrays, such as those used in MIMO operations. Wide beam coverage can also be achieved through the implementation of beam-steering features. However, challenges arise in incorporating these features, as a compact antenna design often leads to strong inter-element coupling.

This study investigates how reducing the spacing between elements in a dual-polarized antenna can minimize mutual coupling and lower sidelobe levels without compromising the directional radiation pattern. A directional radiation pattern typically has a narrow beamwidth; therefore, beam-steering is necessary to provide wider beam coverage, allowing the main beam to be directed toward the desired location for stronger signal reception.

In previous studies, such as in [31], a beam scanning angle of approximately ±63° was achieved using decoupling techniques to reduce mutual coupling. However, the antenna configuration involved a multi-layered structure and dual-probe feeding. The height of a single antenna element was approximately 1.3–1.4 mm. Although this configuration significantly reduced mutual coupling, achieving isolation levels greater than 15 dB, the resulting beam pattern had a narrow beamwidth, indicating reduced directivity.

Similarly, in the study by [32], a complex, multi-layered antenna structure was developed to achieve wide beam coverage. The antenna dimensions were 5.6 × 5.6 × 1.759 mm^3, and it achieved a beam scanning range of 110°, covering 5G millimeter-wave bands n257 and n258, particularly for satellite communications. However, wider beamwidths typically result in lower signal strength, making it difficult to overcome high path loss. This highlights the importance of beam-steering in high-frequency applications to ensure high-quality signal transmission.

The study by [33] proposed a single-layer, dual-polarized antenna with a thickness of 1.5 mm, achieving a beam scanning angle of approximately 79°. However, it required two transmission lines to excite the dual-polarization signals.

In comparison to the aforementioned studies, this research explores a simpler dual-polarized antenna for the millimeter-wave frequency band using only a single layer and a single feeding port and enhancing the antenna performance by reducing the inter-elements spacing. The design mitigates high path loss through a directional main beam while simultaneously providing wide beam coverage by implementing beam-steering. The proposed antenna element has been configured into a linear array to observe its mutual coupling performance. A comparison between the previous studies and this work has been summarized in the Table 5 below.

Table 5 *The summary comparison between the previous studies and this work*

Studies	Antenna structure	Height dimension (mm)	No. of feeding probe port(s)	Mutual coupling (dB)	Beamwidth
[31]	Multi-layered	1.3	2	<-10	60°/45°
[32]	Multi-layered	1.7	2	<-40	110°
[33]	Single-layered	1.5	2	<-15	79°
This work	Single-layered	1.5	1	<-20	40°

5. Conclusion

This study successfully demonstrates the development of a compact, single-layer, dual-polarized slant ±45° patch antenna with reduced inter-element spacing, optimized for 5G millimeter-wave applications at 28 GHz. The inter-elements spacing is reduced from approximately 57 mm to 15 mm. The proposed design, utilizing a Rogers RT5880 substrate and a T-power divider, exhibits improved performance in terms of reflection coefficient, radiation patterns, and gain. The measured reflection coefficient remains below -10 dB, and the radiation patterns achieve gains ranging from 3.7 to 7.8 dBi. Additionally, the improved antenna exhibits reduced sidelobes and a more directional main beam in the co-elevation azimuth pattern compared to previous design [21]. These enhancements make the antenna a strong candidate for 5G millimeter-wave applications, particularly in beam-steering systems. Future research could further explore its integration into adaptive beamforming networks and phased array systems to enhance wireless communication efficiency.

Acknowledgement

The dissemination of this work was supported in part by the Ministry of Higher Education, Malaysia under Grant FRGS/1/2024/TK08/UIAM/02/1.

Conflict of Interest

Authors declare that there is no conflict of interests regarding the publication of the paper.

Author Contribution

All authors reviewed the results and approved the final version of the manuscript.

References

[1] A. Bagheri, M. Khodadadi, T. Brown, P. Xiao, and M. Khalily, "Single-feed, dual-polarized transmissive metasurface antenna for 5G applications," *AEU - International Journal of Electronics and Communications*, vol. 191, p. 155652, 2025, doi: https://doi.org/10.1016/j.aeue.2024.155652.

[2] P. Tiwari, V. Gahlaut, M. Kaushik, P. Rani, A. Shastri, and B. Singh, "Advancing 5G Connectivity: A Comprehensive Review of MIMO Antennas for 5G Applications," *Int J Antennas Propag*, vol. 2023, no. 1, p. 5906721, Jan. 2023, doi: https://doi.org/10.1155/2023/5906721.

[3] P. Sundaravadivel, D. R. Kumar, Y. Padmanaban, and O. P. Kumar, "A versatile conformal circularly polarized quad-element antenna for X-band applications," *Sci Rep*, vol. 14, no. 1, p. 27721, 2024, doi: 10.1038/s41598-024-79197-2.

[4] S. N. R. Rizvi *et al.*, "Isolation enhancement of a capacitively-fed MIMO antenna using a quasi-fractal parasitic element and defected ground structure," *Heliyon*, vol. 10, no. 20, p. e39228, 2024, doi: https://doi.org/10.1016/j.heliyon.2024.e39228.

[5] Y. He, W. Tian, J. Qiao, and L. Zhang, "A compact broadband dual-polarized antenna element for 2G/3G/4G base station applications," in *12th European Conference on Antennas and Propagation (EuCAP 2018)*, 2018, pp. 1–4. doi: 10.1049/cp.2018.0369.

[6] R. Vadlamudi and D. S. Kumar, "Dual Band, Dual Slant $\pm 45^{\circ}$ Polarized 2×2 MIMO (8T 8R) Antenna Array with Low Mutual Coupling for A-LTE(4G) Band 41/42/43(5G) BTS Application," in *2020 International Conference on Wireless Communications Signal Processing and Networking (WiSPNET)*, 2020, pp. 97–101. doi: 10.1109/WiSPNET48689.2020.9198541.

[7] L. Vallozzi, "Patch antenna with slanted ±45° dual polarization and performance comparison with H/V diversity," in *2016 10th European Conference on Antennas and Propagation (EuCAP)*, 2016, pp. 1–5. doi: 10.1109/EuCAP.2016.7481907.

[8] N. O. Parchin, A. Ullah, H. J. Basherlou, R. A. Abd-Alhameed, E. M. I. Elfoghi, and M. S. A. Alkhambashi, "Dual-Polarized Array Antenna with Quasi-End-Fire Radiation for 28 GHz 5G Mobile Terminals," in *IMDC-SDSP 2020: Proceedings of the 1st International Multi-Disciplinary Conference Theme: Sustainable Development and Smart Planning, IMDC-SDSP 2020, Cyperspace, 28-30 June 202*, European Alliance for Innovation, 2020, p. 241.

[9] J. Park, D. Choi, and W. Hong, "28 GHz 5G dual-polarized end-fire antenna with electrically-small profile," 2018.

[10] C. Di Paola, K. Zhao, G. F. Pedersen, and S. Zhang, "Multi-mode dual-polarised cavity backed patch antenna array for 5G mobile devices," *IET Microwaves, Antennas & Propagation*, vol. 15, no. 3, pp. 280–288, 2021.

[11] V. F. Fusco and P. H. Rao, "Wide-band dual slant linearly polarized antenna," *IEEE Trans Antennas Propag*, vol. 51, no. 8, pp. 2014–2019, 2003.

[12] K. Surmeli and A. Kizilay, "Design of slant polariser for directional antennas and antenna arrays," *IET Microwaves, Antennas & Propagation*, vol. 13, no. 10, pp. 1546–1553, 2019.

[13] H. Zhang, D. Ding, and X. Y. Zhang, "Broadband dual-polarized antenna with stable radiation patterns for base station applications," *IEEE Antennas Wirel Propag Lett*, vol. 22, no. 2, pp. 337–341, 2022.

[14] M. Ciydem and E. A. Miran, "Dual-polarization wideband sub-6 GHz suspended patch antenna for 5G base station," *IEEE Antennas Wirel Propag Lett*, vol. 19, no. 7, pp. 1142–1146, 2020.

[15] F.-C. Chen, Y.-Z. Liang, W.-F. Zeng, and K.-R. Xiang, "A Series-Fed Slant-Polarized Microstrip Patch Antenna Array," *IEEE Trans Antennas Propag*, 2024.

[16] L. Kang, H. Li, B. Tang, X. Wang, and J. Zhou, "Quad-polarization-reconfigurable antenna with a compact and switchable feed," *IEEE Antennas Wirel Propag Lett*, vol. 20, no. 4, pp. 548–552, 2021.

[17] K. M. Mak, H. W. Lai, and K. M. Luk, "A 5G wideband patch antenna with antisymmetric L-shaped probe feeds," *IEEE Trans Antennas Propag*, vol. 66, no. 2, pp. 957–961, 2017.

[18] J.-C. S. Chieh, E. Yeo, M. Kerber, R. Olsen, E. Merulla, and S. Sharma, "A 28 GHz Dual Slant Polarized Phased Array using Silicon Beamforming Chipsets," in *2019 IEEE International Symposium on Phased Array System & Technology (PAST)*, 2019, pp. 1–5. doi: 10.1109/PAST43306.2019.9020837.

[19] J. H. Bae and Y. J. Yoon, "5G Dual (S-/Ka-) Band Antenna Using Thick Patch Containing Slotted Cavity Array," *IEEE Antennas Wirel Propag Lett*, vol. 20, no. 6, pp. 1008–1012, 2021, doi: 10.1109/LAWP.2021.3069709.

[20] Q. Yang, S. Gao, L. Wen, X. Ren, D. Kong, and W. Liu, "±45° Linearly Polarized Slot-Coupled Patch Antenna for Millimeter-Wave Applications," in *2020 9th Asia-Pacific Conference on Antennas and Propagation (APCAP)*, 2020, pp. 1–2. doi: 10.1109/APCAP50217.2020.9246023.

[21] S. Z. Mohd Hamzah, N. F. Abdul Malek, S. Y. Mohamad, and F. N. Mohd Isa, "Design and Fabrication of High-Gain Dual Linearly Polarized Patch antenna at 28 GHz," *J Phys Conf Ser*, vol. 2922, no. 1, p. 012005, 2024, doi: 10.1088/1742-6596/2922/1/012005.

[22] Q. Lv, Y.-H. Yang, S.-G. Zhou, C. Shao, D. Zhou, and C.-Y.-D. Sim, "Design of a single-layer±45° dual-polarized directional array antenna for millimeter wave applications," *Sensors*, vol. 21, no. 13, p. 4326, 2021.

[23] Y.-H. Yang, S.-G. Zhou, and Y.-L. Dong, "A Single-Layer ± 45° Dual-Polarized Array Antenna Based on Phase Control Approach," in *2020 International Symposium on Antennas and Propagation (ISAP)*, 2021, pp. 245–246. doi: 10.23919/ISAP47053.2021.9391383.

[24] A. Tiwari, U. Pattapu, and S. Das, *A wideband 1:2 T-junction power divider for antenna array with optimum results*. 2018. doi: 10.1109/ICMAP.2018.8354594.

[25] Y. A. Rayisiwi and T. Hariyadi, "Design of A 1: 12 power divider at 5 GHz for ground surveillance radar application," in *IOP Conference Series: Materials Science and Engineering*, IOP Publishing, 2018, p. 012053.

[26] S. Sotyohadi, I. K. Somawirata, K. A. Widodo, S. T. Phung, and I. Zekker, "Design and Simulation 'Ha'-Slot Patch Array Microstrip Antenna for WLAN 2.4 GHz: Ivar Zekker3," *Proceedings of the Pakistan Academy of Sciences: A. Physical and Computational Sciences*, vol. 58, no. S, pp. 109–117, 2021.

[27] T. Hong, S. Zheng, R. Liu, and W. Zhao, "Design of mmWave directional antenna for enhanced 5G broadcasting coverage," *Sensors*, vol. 21, no. 3, p. 746, 2021.

[28] N. H. M. Adnan, I. M. Rafiqul, and A. H. M. Z. Alam, "Effects of inter-element spacing and number of elements on planar array antenna characteristics," *Indonesian Journal of Electrical Engineering and Computer Science (IJEECS)*, vol. 10, no. 1, 2018.

[29] K. O. Ballagh, "Calibration of an anechoic room," *J Sound Vib*, vol. 105, no. 2, pp. 233–241, 1986, doi: https://doi.org/10.1016/0022-460X(86)90152-5.

[30] E. Steven W, "Electromagnetics Vol 2," 2020.

[31] Y. He, S. Lv, L. Zhao, G.-L. Huang, X. Chen, and W. Lin, "A Compact Dual-Band and Dual-Polarized Millimeter-Wave Beam Scanning Antenna Array for 5G Mobile Terminals," *IEEE Access*, vol. 9, pp. 109042–109052, 2021, doi: 10.1109/ACCESS.2021.3100933.

[32] Z. Wang, Z. Pan, X. Zhao, J. Sheng, Y. Hu, and W. Hong, "A Wideband Dual-Polarized Antenna with Wide Beam for Millimeter-Wave Applications," in *2023 IEEE 11th Asia-Pacific Conference on Antennas and Propagation (APCAP)*, 2023, pp. 1–2. doi: 10.1109/APCAP59480.2023.10470307.

[33] Y. Zhu, Y. Hao, and C. Deng, "Single-Layer Dual-Polarized End-Fire Phased Array Antenna for Low-Cost Millimeter-Wave Mobile Terminal Applications," in *2022 IEEE Conference on Antenna Measurements and Applications (CAMA)*, 2022, pp. 1–3. doi: 10.1109/CAMA56352.2022.10002551.